Inorganic Chemistry

Article

pubs.acs.org/IC

Combination of Magnetic Susceptibility and Electron Paramagnetic Resonance to Monitor the 1D to 2D Solid State Transformation in Flexible Metal–Organic Frameworks of Co(II) and Zn(II) with 1,4-Bis(triazol-1-ylmethyl)benzene

Eugenio Coronado, Mónica Giménez-Marqués, and Guillermo Mínguez Espallargas*

Instituto de Ciencia Molecular (ICMol), Universidad de Valencia, c/Catedrático José Beltrán, 2, 46980 Paterna, Spain

Supporting Information

ABSTRACT: Two families of coordination polymers, $\{[M(btix)_2(OH_2)_2]\cdot 2NO_3\cdot 2H_2O\}_n$ [M = Co (**1**), Zn (**2**), Co–Zn (**3**); btix = 1,4-bis(triazol-1-ylmethyl)benzene] and $\{[M(btix)_2(NO_3)_2]\}_n$ [M = Co (**4**), Zn (**5**), Co–Zn (**6**)], have been synthesized and characterized. The two conformations of the ligand, *syn* and *anti*, lead to one-dimensional (1D) cationic chains or two-dimensional (2D) neutral grids. Extrusion of the water molecules of the 1D compounds results in an irreversible transformation into the 2D compounds, which involves a change in conformation of the btix ligands and a rearrangement in the metal environment with cleavage and reformation of covalent bonds. This structural transformation has been followed by electron paramagnetic resonance (EPR) and magnetic susceptibility measurements to monitor the minor modifications that the metal centers suffer.

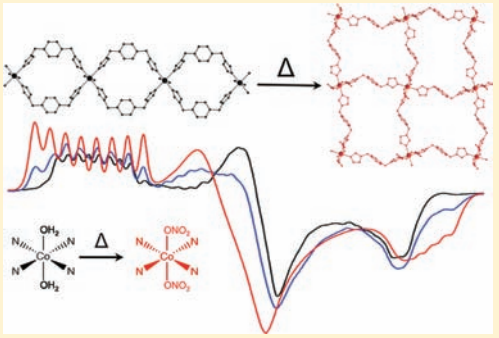

INTRODUCTION

Metal–Organic Frameworks (MOFs) are porous coordination polymers composed of metal ions or metal clusters as nodes and multitopic organic ligands as linkers.[1,2] These compounds have potential applications that cover from catalysis and separations of mixtures, to gas storage media for sensors and electronic devices.[2,3] The most common strategy for the synthesis of MOFs involves the use of rigid ligands to bridge between the metal nodes leading to robust frameworks.[4] However, there is a growing interest in the search for flexible and dynamic MOFs owing to their potential applications as functional materials.[5,6] Several examples of "breathing" MOFs are known, in which structural changes occur upon guest removal/inclusion without bond cleavage, implying that the framework retains the same (or similar) topology.[7,8] However, examples of solid state transformations that involve formation and cleavage of covalent bonds, while maintaining the crystallinity, are less common.[9] In these cases a drastic rearrangement of the network connectivity can occur, with changes in ligand coordination which affect the dimensionality of the network and can influence the physical properties of the coordination polymer.[10,11] Single-crystal-to-single-crystal transformations are the most desirable of these reactions, since they permit the unequivocal structural characterization of the product.[12,13] However, large atomic motions can provoke breaks in the single crystals and often yields a polycrystalline powder that can hinder the structural characterization, thus disabling complete comprehension of the changes in the properties of the material. Recent improvements on X-ray powder diffraction (XRPD) analysis have permitted the ab initio structural determination of MOFs after structural transformation,[6b,14] although it can be very challenging because of the high complexity of these systems. Spectroscopic techniques and thermoanalytical methods also provide useful information on the structural rearrangement,[13] and molecular dynamic simulations have also been reported to confirm the movement of a flexible fragment for which a suitable model from X-ray powder data could not be obtained.[15]

Magnetic MOFs are attracting increasing attention in the field of molecular magnetism because their magnetic properties can be modified by the structural changes provoked by the uptake of molecular species in the pores, making them suitable candidates for potential application as switches or sensors.[16] In addition, the presence of magnetic centers permits the application of electron paramagnetic resonance (EPR) and magnetic susceptibility to gather information on structural features. EPR can provide information on the changes of the coordination sphere of the metal, whereas magnetic susceptibility measurements can help to elucidate the connectivity between the metal centers. This kind of magneto-structural correlations has been extensively applied to molecular coordination complexes in the early years of molecular magnetism,[17] but its application in flexible MOFs is novel. In this paper we show that EPR and magnetic susceptibility measurements can be very useful to monitor structural

Received: February 6, 2012
Published: March 19, 2012

   dx.doi.org/10.1021/ic300276q | *Inorg. Chem.* 2012, 51, 4403–4410

Table 1. Crystallographic Data for Compounds 1, 2, 4, and 5

	1	2	4	5
empirical formula	$C_{24}H_{32}N_{14}O_{10}Co$	$C_{24}H_{32}N_{14}O_{10}Zn$	$C_{24}H_{24}N_{14}O_6Co$	$C_{24}H_{24}N_{14}O_6Zn$
formula weight	735.57	742.01	663.50	669.94
crystal color	pink	colorless	pink	colorless
crystal size (mm^3)	0.10 × 0.10 × 0.10	0.20 × 0.10 × 0.10	0.14 × 0.12 × 0.04	0.16 × 0.08 × 0.04
temperature (K)	120(2)	120(2)	120(2)	120(2)
crystal system, Z	triclinic, 1	triclinic, 1	monoclinic, 2	monoclinic, 2
space group	$P\bar{1}$	$P\bar{1}$	$P2_1/c$	$P2_1/c$
a (Å)	9.0395(10)	9.0695(7)	8.2019(5)	8.1968(3)
b (Å)	9.3091(10)	9.3491(7)	20.7198(11)	20.7210(9)
c (Å)	10.5172(12)	10.5511(8)	8.4751(5)	8.4639(3)
α (deg)	80.840(9)	80.933(6)	90	90
β (deg)	76.092(10)	75.831(7)	105.604(6)	105.358(4)
γ (deg)	61.651(11)	61.733(8)	90	90
V ($Å^3$)	754.99(14)	763.08(10)	1387.19(14)	1386.22(9)
ρ_{calc} (Mg/m^3)	1.618	1.615	1.588	1.605
$\mu(Mo_{K\alpha})$ (mm^{-1})	0.650	0.885	0.688	0.955
θ range (deg)	2.61−27.57	2.48−29.13	2.58−27.53	1.97−27.50
reflns collected	10922	17419	10941	9927
independent reflns (R_{int})	3232 (0.0865)	4114 (0.0858)	3176 (0.0642)	3172 (0.0489)
reflns used in refinement, n	3232	4114	3176	3172
L. S. parameters, p/ restraints, r	233/4	263/4	200/0	233/0
$R1(F)$,[a] $I > 2\sigma(I)$	0.0538	0.0394	0.0378	0.0422
$wR2(F^2)$,[b] all data	0.1245	0.0599	0.0624	0.0860
$S(F^2)$,[c] all data	0.964	0.777	0.785	1.141

[a] $R1(F) = \sum||F_o| - |F_c||/\sum|F_o|$. [b] $wR2(F^2) = [\sum w(F_o^2 - F_c^2)^2/\sum wF_o^4]^{1/2}$. [c] $S(F^2) = [\sum w(F_o^2 - F_c^2)^2/(n + r - p)]^{1/2}$.

transformations in flexible magnetic MOFs that involve cleavage and formation of covalent bonds with a change in the dimensionality of the system.

EXPERIMENTAL SECTION

Synthesis. The ligand 1,4-bis(triazol-1-ylmethyl)benzene (btix) was prepared according to a literature method with some modifications.[18] All reagents and solvents were commercially available and used without further purification.

Synthesis of $\{[Co(btix)_2(OH_2)_2]\cdot 2NO_3\cdot 2H_2O\}_n$ ***(1)***. A solution of $Co(NO_3)_2\cdot 6H_2O$ (125.2 mg, 0.4 mmol) in 4 mL of H_2O was added slowly into a EtOH/H_2O solution (7:1 v/v) of btix (96.0 mg, 0.4 mmol) without stirring. The mixture was left at room temperature (RT) for crystallization. After several days, pink needle-shaped crystals were filtered off and washed with water. Phase purity was established by XRPD. Yield 82%. Anal. Calcd $C_{24}H_{32}CoN_{14}O_{10}$ (735.54): C, 39.19; H, 4.39; N, 26.66%. Found: C, 39.11; H, 4.39; N, 25.97%.

Synthesis of $\{[Zn(btix)_2(OH_2)_2]\cdot 2NO_3\cdot 2H_2O\}_n$ ***(2)***. **2** was synthesized in a procedure analogous to that of **1** except that $Zn(NO_3)_2\cdot 6H_2O$ (120.0 mg, 0.4 mmol) was used instead of $Co(NO_3)_2\cdot 6H_2O$. Colorless block-shaped crystals were filtered off and washed with water. Yield 67%. Anal. Calcd $C_{24}H_{32}ZnN_{14}O_{10}$ (742.00): C, 38.85; H, 4.35; N, 26.43%. Found: C, 38.90; H, 4.32; N, 25.89%.

Synthesis of $\{[Zn_{(0.98)}Co_{(0.02)}(btix)_2(OH_2)_2]\cdot 2NO_3\cdot 2H_2O\}_n$ ***(3)***. **3** was synthesized in a procedure analogous to that of **1** except that a mixture of $Zn(NO_3)_2\cdot 6H_2O$ (116.6 mg, 0.392 mmol) and $Co(NO_3)_2\cdot 6H_2O$ (2.4 mg, 0.008 mmol) was used. Light-pink needle-shaped crystals were filtered off and washed with water. Yield 80%. Phase purity was established by XRPD.

Synthesis of $[Co(btix)_2(NO_3)_2]_n$ ***(4)***. Different routes are available for the synthesis of **4**. Crystals of **1** were heated to 353 K for 2 h to yield **4** as pale pink crystalline powder (yield 100%.). Alternatively, **4** can be obtained by slow addition of a solution of $Co(NO_3)_2\cdot 6H_2O$ (125.2 mg, 0.4 mmol) in 15 mL of MeOH into a solution of btix (96.0 mg, 0.4 mmol) in 20 mL of MeOH without stirring. The mixture was left at RT for crystallization. After filtration, pink needle-shaped crystals were obtained in 24 h and washed with MeOH. Phase purity was established by XRPD. Yield 94%. Anal. Calcd $C_{24}H_{24}CoN_{14}O_6$ (663.48): C, 43.45; H, 3.65; N, 29.56%. Found: C, 42.77; H, 3.84; N, 28.32%.

Synthesis of $[Zn(btix)_2(NO_3)_2]_n$ ***(5)***. **5** was synthesized in a procedure analogous to that of **4** except that $Zn(NO_3)_2\cdot 6H_2O$ (120.0 mg, 0.4 mmol) was used instead. Colorless block-shaped crystals were filtered off and washed with MeOH. Yield 87%. Anal. Calcd $C_{24}H_{24}ZnN_{14}O_6$ (669.94): C, 42.52; H, 4.76; N, 28.92%. Found: C, 42.66; H, 3.64; N, 28.74%.

Synthesis of $[Zn_{(0.98)}Co_{(0.02)}(btix)_2(NO_3)_2]_n$ ***(6)***. **6** was synthesized in a procedure analogous to that of **4** except that a mixture of $Zn(NO_3)_2\cdot 6H_2O$ (116.6 mg, 0.392 mmol) and $Co(NO_3)_2\cdot 6H_2O$ (2.4 mg, 0.008 mmol) was used. Light-pink block-shaped crystals were filtered off and washed with MeOH. Yield 83%. Phase purity was established by XRPD.

X-ray Structural Studies. Single crystals of compounds **1**, **2**, **4**, and **5** were mounted on glass fibers using a viscous hydrocarbon oil to coat the crystal and then transferred directly to the cold nitrogen stream for data collection. X-ray data were collected at 120 K on a Supernova diffractometer equipped with a graphite-monochromated Enhance (Mo) X-ray Source (λ = 0.71073 Å). The program CrysAlisPro, Oxford Diffraction Ltd., was used for unit cell determinations and data reduction. Empirical absorption correction was performed using spherical harmonics, implemented in the SCALE3 ABSPACK scaling algorithm. Crystal structures were solved and refined against all F^2 values using the SHELXTL suite of programs.[19] Non-hydrogen atoms were refined anisotropically (except the disordered fragments) and hydrogen atoms were placed in calculated positions that were refined using idealized geometries (riding model) and assigned fixed isotropic displacement parameters except for those of water molecules, which were located and refined with distance restraints. In **1** and **2**, the (noncoordinated) NO_3^- anions are disordered over two sites and have been modeled with 51.2(13):48.8(13) and 62(4):38(4) ratios respectively. In **4** and **5**, the (coordinated) NO_3^- anions are disordered over two sites and have been modeled with 51.9(3):48.1(3) and 51.2(4):48.8(4) ratios respectively. In addition, the benzene moiety of the btix ligand in compound **4** is disordered over two sites and have been modeled with

dx.doi.org/10.1021/ic300276q | Inorg. Chem. 2012, 51, 4403−4410

a 53.2(19):46.8(19) ratio. A summary of the data collection and structure refinements is provided in Table 1. CCDC-865645 (**1**), -865646 (**2**), -865647 (4), and -865648 (**5**) contain the supplementary crystallographic data for this paper. These data can be obtained free of charge from The Cambridge Crystallographic Data Centre via www.ccdc.cam.ac.uk/data_request/cif.

XRPD Measurements. Polycrystalline samples of **1**, **3**, **4**, and **6** were lightly ground in an agate mortar and pestle and filled into 0.7 mm borosilicate capillaries. Data were collected at RT in the 2θ range 0−30° on a Supernova diffractometer equipped with a graphite-monochromated Enhance (Mo) X-ray Source (λ = 0.71073 Å) (**1**, **4**, **6**) and in the 2θ range 0−40° on an Xcalibur S Gemini diffractometer equipped with Cu X-ray Source (λ = 1.54056 Å) (**3**).

Thermogravimetric Analysis. Thermogravimetric analysis of **1** and **4** were carried out with a Mettler Toledo TGA/SDTA 851 apparatus in the 25−800 °C temperature range under a 10 °C·min^{-1} scan rate and an air flow of 30 mL·min^{-1}. In addition, thermogravimetric analysis of compound **1** was also performed at a fixed temperature of 80 °C. Thermogravimetric analysis of **1** shows a mass loss of 10.6% between 70 and 120 °C, which corresponds to removal of four water molecules per formula unit (calculated 11.5%) whereas compound **4** remains stable until 280 °C and then decomposes. Gravimetric analysis of compound **1** at a constant temperature of 80 °C shows a total loss of weight of 10.9% after 10 min of heating, which corresponds to the loss of four water molecules per formula unit (calculated 11.5%), and remains stable afterward.

Magnetic Measurements. Magnetic susceptibility measurements were performed on single-phased polycrystalline samples of **1** and **4** with a Quantum Design SQUID magnetometer. The susceptibility data were corrected from the diamagnetic contributions as deduced by using Pascal's constant tables. The direct current (d.c.) data were collected in the range 2−300 K for decreasing temperatures with an applied field of 1000 G. Electron paramagnetic resonance spectroscopy was recorded with a Bruker ELEXYS E580 spectrometer operating in the X-band (9.47 GHz).

RESULTS AND DISCUSSION

Six MOFs based on the flexible ligand 1,4-bis(triazol-1-ylmethyl)benzene (btix) have been prepared by slow evaporation of the solvent at RT and two different families have been synthesized depending on the choice of the solvent. The ligand can adopt two different conformations, *syn* and *anti* (Figure 1), because of the presence of methylene groups

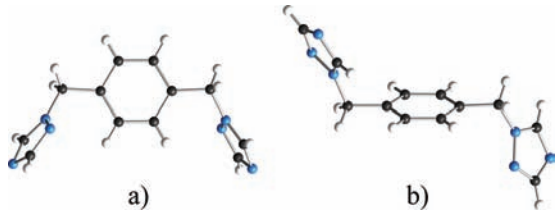

Figure 1. Conformations of the flexible ligand btix: (a) *syn*; (b) *anti*.

between the triazole and the benzene rings, which leads to different coordination frameworks.[20,21]

The reaction of $M(NO_3)_2{\cdot}6H_2O$ (M = Co^{II}, Zn^{II}) and btix in a EtOH/H_2O solution results in the formation of block-shaped crystals of formula $\{[M(btix)_2(OH_2)_2]{\cdot}2NO_3{\cdot}2H_2O\}_n$ [M = Co (**1**),[20] Zn (**2**), Co−Zn (**3**)]. Crystallographic analysis reveals that compounds **1**, **2**, and **3** are composed of one-dimensional (1D) chains that run parallel to the crystallographic $10\bar{1}$ direction (Figure 2). They crystallize in the triclinic $P\bar{1}$ space group. The asymmetric unit consists of one crystallographically independent M^{II} that lies in the inversion center with *trans*-N4O2 coordination octahedron mode. Each metal is

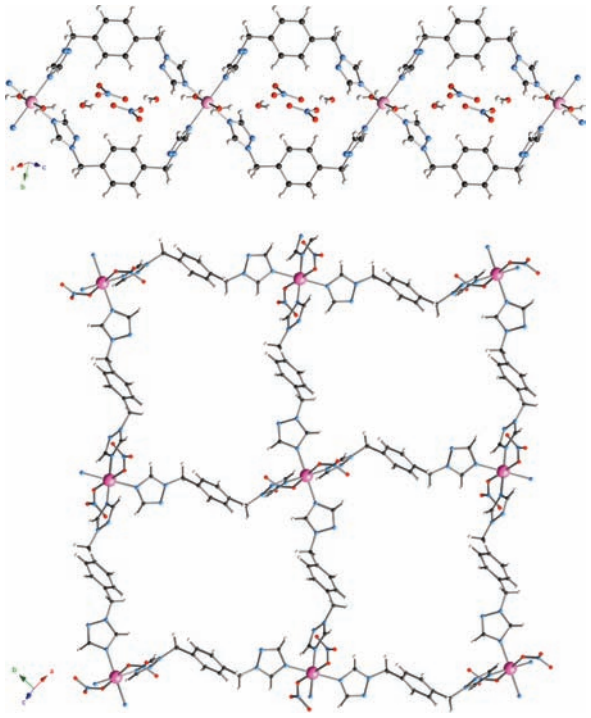

Figure 2. Crystal structures of compounds **1** (top) and **4** (bottom). Cobalt, nitrogen, oxygen, carbon, and hydrogen are colored pink, blue, red, black, and white, respectively. Compounds **2** and **3** are isostructural to **1**, and compounds **5** and **6** are isostructural to **4**.

coordinated by four triazole nitrogen atoms derived from four *syn*-btix ligands in the equatorial positions and two oxygen atoms from water molecules in the apical positions. The coordination environment of the M^{II} ions features a slightly distorted octahedron with Co−N distances of 2.137(3) and 2.162(3) Å and Co−O distance of 2.094(2) Å for compound **1**, and Zn−N distances of 2.140(2) and 2.173(2) Å and Zn−O distances of 2.1295(14) Å for compound **2**, and angles that slightly deviate from idealized octahedron geometry (see Table 2). Two *syn*-btix ligands act as bridges between adjacent metal centers leading to M···M distances of 12.1087(17) and 12.1134(11) Å for **1** and **2**, respectively.

The 1D networks are cationic, and the charge is compensated by the presence of NO_3^- anions in the voids (Figure 2). In addition, the voids are filled with water molecules which complete a hydrogen bonding network that involves both the coordinated and noncoordinated water molecules and the nitrate anions (see Figure 3).

The reaction of $M(NO_3)_2{\cdot}6H_2O$ (M = Co^{II}, Zn^{II}) and btix in MeOH results in the formation of block-shaped crystals of formula $\{[M(btix)_2(NO_3)_2]\}_n$ [M = Co (**4**),[20] Zn (**5**), Co−Zn (**6**)]. Compounds **4**, **5**, and **6** crystallize in the monoclinic $P2_1/c$ space group. Each metal lies in an inversion center and is coordinated by four triazole nitrogen atoms from four *anti*-btix ligands and two oxygen atoms from two nitrate ions in the apical positions (Figure 2). Thus, the coordination sphere of each M^{II} ion is very similar to those of **1**−**3**, with *trans*-N4O2 coordination octahedron mode. The Co−N distances are 2.121(2) and 2.137(2) Å and the Co−O distances are 2.192(3) and 2.154(3) Å for the two disordered NO_3^- anions for compound **4**, and the Zn−N distances are 2.143(2) and 2.119(2) Å and the Zn−O distances are 2.223(4) and 2.190(3) Å for the two disordered NO_3^- anions for compound **5**. The

dx.doi.org/10.1021/ic300276q | Inorg. Chem. 2012, 51, 4403−4410

Table 2. Selected Bond Lengths and Angles for 1, 2, 4, and 5

	1	2	4	5
M–N (Å)	2.137(3)	2.140(2)	2.121(2)	2.143(2)
	2.162(3)	2.173(2)	2.137(2)	2.119(2)
M–O (Å)	2.094(2)	2.1295(14)	2.192(3)[a]	2.223(4)[c]
			2.154(3)[b]	2.190(3)[d]
N–M–N (deg)	92.72(10)	93.39(6)	90.35(6)	90.18(7)
	180	180	180	180
N–M–O (deg)	92.07(10)	92.15(6)	91.32(9)[a]	90.90(12)[c]
	92.08(9)	91.93(6)	102.08(10)[a]	102.29(13)[c]
			97.25(8)[b]	97.67(10)[d]
			102.26(10)[b]	102.22(12)[d]
O–M–O (deg)	180	180	180[a]	180[c]
			180[b]	180[d]

[a]This value corresponds to the NO_3^- anion with 48.1(3) % occupancy. [b]This value corresponds to the NO_3^- anion with 51.9(3) % occupancy. [c]This value corresponds to the NO_3^- anion with 51.2(4) % occupancy. [d]This value corresponds to the NO_3^- anion with 48.8(4) % occupancy.

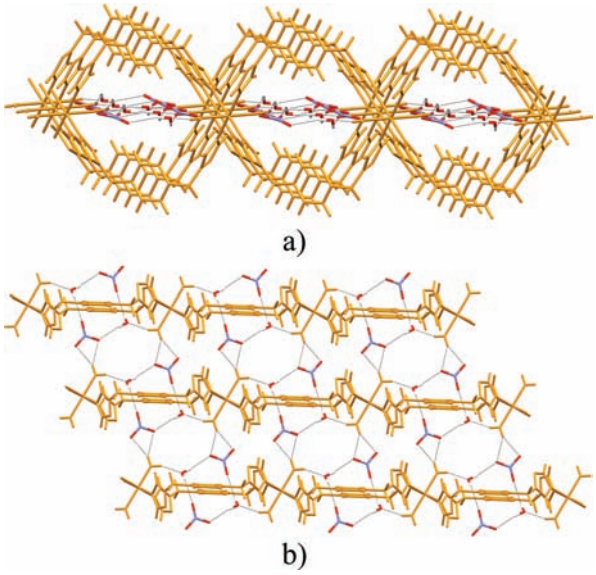

Figure 3. (a) 1D chains formed by **1**–**3** that run parallel to the crystallographic $10\bar{1}$ direction; the voids are filled with noncoordinated water molecules and nitrate anions. (b) Hydrogen bonding network formed by both the coordinated and the noncoordinated water molecules and the nitrate anions. The cationic 1D networks are represented in orange while nitrogen, oxygen and hydrogen from nitrate and noncoordinated water molecules are colored blue, red, and white, respectively. Black dotted lines represent hydrogen bonds.

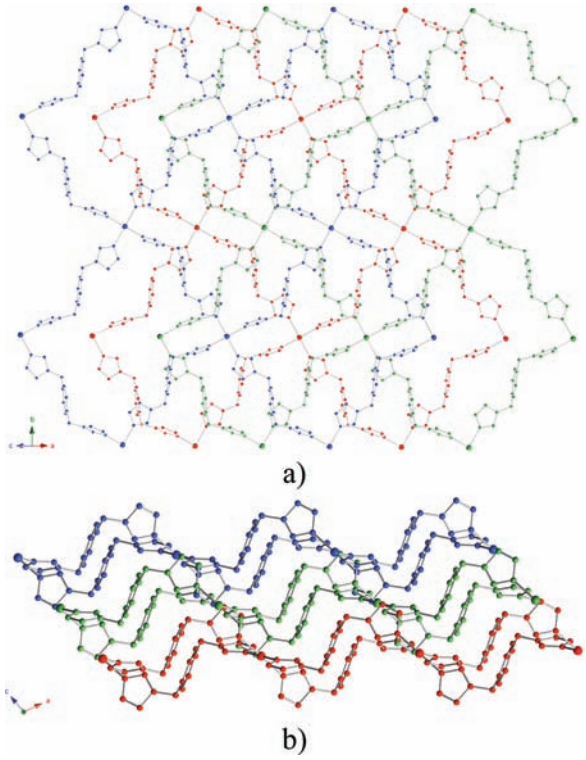

Figure 4. Crystal structure of compounds **4**–**6** showing the 2D grids with (4,4) topology stacking along the 101 axis in an ABCABC fashion, shown in two orientations (top and bottom) which are related by rotation of 90° of the 101 axis. Red, green and blue represent three different ABC layers. Hydrogen atoms and nitrate ligands have been omitted for clarity.

angles slightly deviate from idealized octahedron geometry (see Table 2). The *anti*-btix ligands act as bidentate linkers generating a 2D grid with (4,4) topology with M···M distances of 14.5346(6) and 14.5193(4) Å for **4** and **5**, respectively. Theses layers stack along the 101 axis in an ABCABC fashion (Figure 4). Weak C–H···O interlayer interactions are observed between the three oxygen atoms of the nitrate anions from one sheet and aromatic and aliphatic C–H groups of the ligand from the next sheet.

The presence of voids in compounds **1**–**3** prompted us to explore whether these channels could be desolvated to obtain a porous MOF suitable for gas uptake. Thermogravimetric analysis of **1** shows a mass loss of 10.6% between 70 and 120 °C, which corresponds to removal of four water molecules per formula unit (expected 11.5%), revealing that both the solvated and the coordinated water molecules in **1** are liberated below 120 °C (Supporting Information, Figure S1). In fact, this loss of water molecules can be achieved by heating **1** at only 80 °C for 1 h (Supporting Information, Figure S2).[22] The XRPD pattern of the dehydrated sample shows that the compound is still crystalline, which implies that the removal of both the solvated and the coordinated water molecules occurs without disrupting the long-range order. However, the diffraction pattern is clearly different from that of the original compound **1** (Figure 5). Thus, a solid-state transformation has occurred during the evacuation process, leading to a different compound. Interestingly, the XRPD pattern of the dehydrated sample corresponds exactly to the XRPD pattern of compound **4**, meaning that the dehydration process is a solid-state reaction in

dx.doi.org/10.1021/ic300276q | *Inorg. Chem.* 2012, 51, 4403–4410

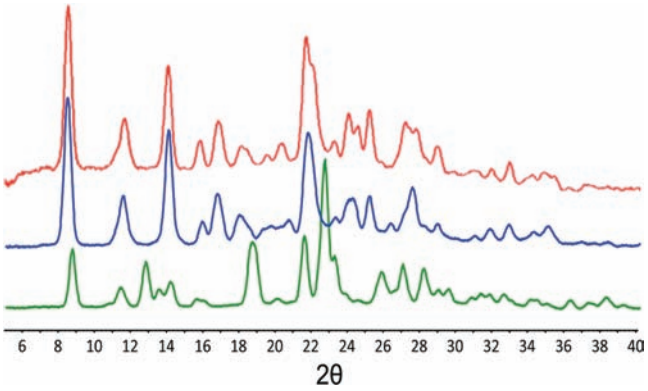

Figure 5. Observed XRPD patterns of **1** before heating (green) and after heating at 80 °C for 1 h (blue), and compound **4** as synthesized (red) (λ = 1.54056 Å).

which **1** is transformed into **4** upon loss of water molecules. This conversion of the chain compound into the 2D compound is remarkable, given the drastic rearrangement of coordination bonds that are needed for this process. Previous reports have shown that topochemical reactions can result in a 1D to 2D structural transformation with minimal movement of atoms.[23] However, the structural transformation **1**→**4** consists of a conformational change of the btix ligand from *syn*-conformation in **1** to *anti*-conformation in **4** and implies the cleavage of coordination bonds between Co^{II} ions and btix ligands, followed by the rotation of btix ligand through the methylene groups to adopt the *anti* conformation and subsequent reformation of Co−N bonds. This rearrangement results in an increase of the dimensionality of the network from 1D to 2D. Additionally, a ligand substitution takes place since the loss of coordinated water molecules is followed by coordination of the NO_3^- anions. Importantly, immersion of compound **4** into water to induce the reversible process, that is, reconversion into **1**, was unsuccessful.

The presence of magnetic centers in these families of MOFs has been exploited to study the structural changes experienced by these solids. More precisely, we have used magnetic susceptibility measurements to study whether the change in metal connectivity (from 1D to 2D) has some influence on the magnetic dimensionality. In addition, EPR spectroscopy has been used to detect changes in the coordination sphere of the metal ion because of its strong sensitivity to the coordination environment of the metal centers.

The product of the molar magnetic susceptibility and temperature, $\chi_M T$, of the Co^{II} compounds (**1** and **4**) are shown in Figure 6. At RT $\chi_M T$ has a value of 3.12 and 3.38 emu K mol^{-1} for **1** and **4**, respectively, and decreases on cooling reaching a minimum value at 2 K of 2.17 and 1.90 emu K mol^{-1} for **1** and **4**, respectively. This decrease is similar in both cases and indicates that the Co−Co exchange interactions are very weak in both compounds, being totally insensitive to the different conformations adopted by the bridging btix ligand (*syn vs anti*). The observed decrease in $\chi_M T$ down to 2 K has to be associated to the single-ion behavior and arises from the depopulation of the excited spin−orbit levels of octahedral Co^{II}. Hence, although the magnetic measurements clearly indicate that the metal centers have a similar connectivity (via the btix ligand), it is insensitive to the different dimensionality of the two networks caused by the change in conformation of the ligand.

The changes in the coordination environments around Co^{II} have been monitored using EPR spectroscopy. Magnetically diluted samples **3** and **6** have been prepared to improve the resolution of the spectra. The EPR spectrum of **3** (Figure 7)

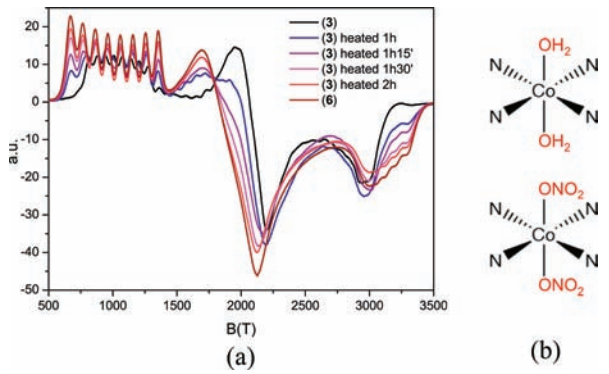

Figure 7. (a) X-band EPR spectra at 4 K of compounds **3** at different times of heating and **6**. (b) Coordination environments of cobalt(II) centers in **3** (top) and **6** (bottom).

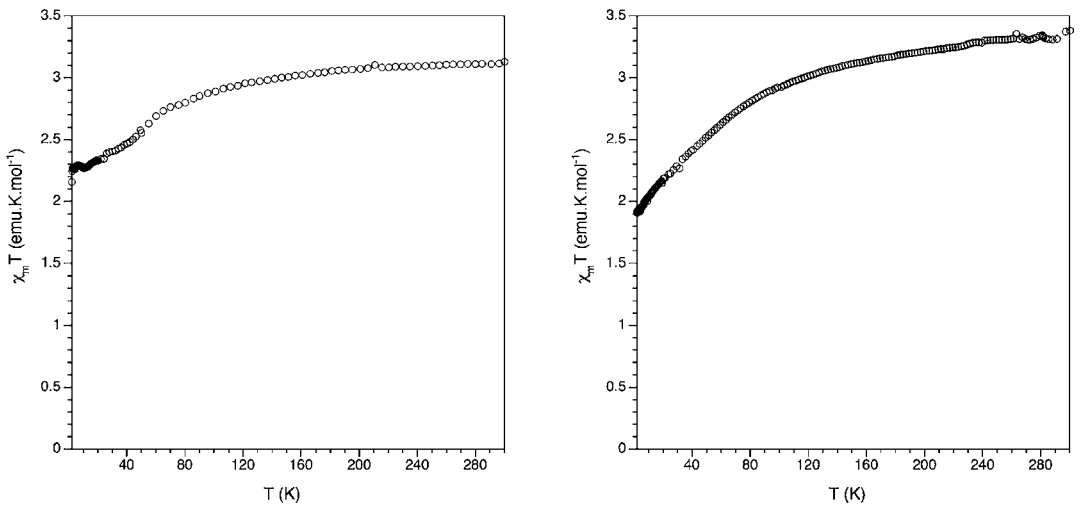

Figure 6. Thermal dependence of the $\chi_M T$ product of **1** (left) and **4** (right) in the temperature range 2−300 K.

dx.doi.org/10.1021/ic300276q | Inorg. Chem. 2012, 51, 4403−4410

displays a typical distorted axial pattern for high-spin Co^{II} with g-values 6.49, 3.28, and 2.31, which is in good agreement with the distorted *trans*-N4O2 coordination octahedron mode observed in the crystallographic analysis.[24] The hyperfine splitting is only apparent on the low-field component, and corresponds to a coupling constant of 65 G for the $I = 7/2$ ^{59}Co nucleus. Upon heating, the EPR spectrum stays unchanged, demonstrating that the coordination environment of the metal is not enormously modified and retains the *trans*-N4O2 coordination octahedron mode. After the solid state transformation, the EPR spectrum remains rhombic, but the g-components slightly change to 6.70, 3.71, and 2.26, indicating the sensitivity to small changes in the coordination environment. In contrast, significant differences are observed in the hyperfine structure of the spectra, with hyperfine constants that increase from 65 (in **3**) to 100 G (in **6**). This is consistent with the modification in the nature of the oxygen ligand, which changes from (neutral) water molecules to (anionic) nitrate ligands (Figure 7b). Thus, EPR spectroscopy is able to detect these minor changes in which the coordination geometry remains similar albeit with changes in the nature of the ligands. To understand the path of the reaction, we have followed the solid-state transformation **3**→**6** by EPR spectroscopy. A sample of **3** was placed in an open capillary and heated at 353 K for 2 h.[25] EPR spectra were recorded every 15 min intervals at 4 K (Figure 7 shows a selection of the EPR spectra). In this way, we were able to quench the reaction and to obtain a sequence of snapshots of the reaction during its progress. It can be observed that the signal corresponding to **3** diminishes in intensity with time, whereas that corresponding to **6** increases, indicating the lack of an intermediate in the reaction. Thus, a concerted substitution reaction in which NO_3^- ligands displace the coordinated H_2O molecules is likely to occur.

CONCLUSIONS

In this work we have reported two families of coordination polymers, $\{[M(btix)_2(OH_2)_2]\cdot 2NO_3\cdot 2H_2O\}_n$ [M = Co (**1**), Zn (**2**), Co−Zn (**3**); btix =1,4-bis(triazol-1-ylmethyl)benzene] and $\{[M(btix)_2(NO_3)_2]\}_n$ [M = Co (**4**), Zn (**5**), Co−Zn (**6**)], where the btix ligand can adopt two different conformations, *syn* and *anti*. The two conformations of the ligand lead to different coordination frameworks. Thus, compounds **1**−**3** consist of non-interpenetrated 1D cationic chains with large cavities that are partially filled with anions and solvent molecules, whereas compounds **4**−**6** form a 2D neutral grid with (4,4) topology. Remarkably, we have shown that the chain compounds are able to extrude both coordinated and nonbonded water molecules and transform into the layered compounds in the solid state upon heating thanks to the flexible btix ligand without loosing their crystallinity. Interestingly, this solid state process involves a change in conformation of the flexible btix ligands (from *syn* to *anti*) and also requires a rearrangement in the metal environment with the cleavage and formation of M−N bonds. In this work we have shown that this structural transformation can be monitored through the use of magnetic techniques as it provokes changes in the magnetic properties of these magnetic MOFs. In particular, these results describe the use of EPR spectroscopy to detect the minor modifications that the Co^{II} coordination sphere suffers upon transformation of the chains to the layer structures, and we are able to follow this transformation without detecting an intermediate in the reaction.

Determination of the structural changes in MOFs is often difficult because of the lack of diffraction data. Here we present a general approach that shows that the presence of magnetic centers can provide very useful information. Thus, this methodology could be applied in more complex systems to better understand solid-state transformations.

ASSOCIATED CONTENT

Supporting Information

Crystallographic data in CIF format. Further details are given in Figures S1−S3. This material is available free of charge via the Internet at http://pubs.acs.org.

AUTHOR INFORMATION

Corresponding Author

*E-mail: guillermo.minguez@uv.es.

Notes

The authors declare no competing financial interest.

ACKNOWLEDGMENTS

The work has been supported by the European Union (Advanced ERC Grant SPINMOL and FP7 Project HINTS), the Spanish Ministerio de Ciencia e Innovacion, MICINN (Project Consolider-Ingenio in Molecular Nanoscience, CSD2007-00010, and projects MAT2007-61584, MAT2011-22785, and CTQ2011-26507), and the Generalitat Valenciana (Prometeo Program). M.G.M. and G.M.E. thank MICINN for a predoctoral grant and a research fellowship (Programa Juan de la Cierva), respectively. We also acknowledge J. M. Clemente-Juan for helpful scientific discussions and J. M. Martíez-Agudo and G. Agustí (University of Valencia) for their help with the magnetic and EPR measurements.

REFERENCES

(1) For reviews on metal−organic frameworks and coordination polymers see: (a) Rowsell, J. L. C.; Yaghi, O. M. *Microporous Mesoporous Mater.* **2004**, *73*, 3. (b) Kitagawa, S.; Kitaura, R.; Noro, S.-i. *Angew. Chem., Int. Ed.* **2004**, *43*, 2334. (c) Suh, M. P.; Cheon, Y. E.; Lee, E. Y. *Coord. Chem. Rev.* **2008**, *252*, 1007. (d) Férey, G. *Chem. Soc. Rev.* **2008**, *37*, 191. (e) James, S. L. *Chem. Soc. Rev.* **2003**, *32*, 276. (f) Janiak, C. *Dalton Trans.* **2003**, 2781. (g) Bradshaw, D.; Claridge, J. B.; Cussen, E. J.; Prior, T. J.; Rosseinsky, M. J. *Acc. Chem. Res.* **2005**, *38*, 273. (h) Cohen, S. M. *Chem. Sci.* **2010**, *1*, 32. (i) Zhao, D.; Timmons, D. J.; Yuan, D.; Zhou, H.-C. *Acc. Chem. Res.* **2011**, *44*, 123. (j) Dincă, M.; Long, J. R. *Angew. Chem., Int. Ed.* **2008**, *47*, 6766. (k) Cheetham, A. K.; Rao, C. N. R.; Feller, R. K. *Chem. Commun.* **2006**, 4780. (l) Champness, N. R. *Dalton Trans.* **2011**, *40*, 10311. (m) Brammer, L. *Chem. Soc. Rev.* **2004**, *33*, 476. (n) Medina, M. E.; Platero-Prats, A. E.; Snejko, N.; Rojas, A.; Monge, A.; Gándara, F.; Gutiérrez-Puebla, E.; Camblor, M. A. *Adv. Mater.* **2011**, *23*, 5283.

(2) See the recent themed issues on Metal−Organic Frameworks: (a) *Chem. Soc. Rev.* **2009**, *38*, 1201−1508. (b) *Chem. Rev.* **2012**, *112*, 673−1268.

(3) (a) Jiang, H.-L.; Xu, Q. *Chem. Commun.* **2011**, *47*, 3351. (b) Maspoch, D.; Ruiz-Molina, D.; Veciana, J. *Chem. Soc. Rev.* **2007**, *36*, 770. (c) Bae, Y.-S.; Snurr, R. Q. *Angew. Chem., Int. Ed.* **2011**, *50*, 11586. (d) Corma, A.; García, H.; Llabrés i Xamena, F. X. *Chem. Rev.* **2010**, *110*, 4606. (e) Chen, B.; Xiang, S.; Qian, G. *Acc. Chem. Res.* **2010**, *43*, 1115.

(4) Representative examples of MOFs using rigid ligands: (a) Eddaoudi, M.; Kim, J.; Rosi, N.; Vodak, D.; Wachter, J.; O'Keeffe, M.; Yaghi, O. M. *Science* **2002**, *295*, 469. (b) Chun, H.; Dybtsev, D. N.; Kim, H.; Kim, K. *Chem.—Eur. J.* **2005**, *11*, 3521. (c) Moulton, B.; Abourahma, H.; Bradner, M. W.; Lu, J.; McManus, G. J.; Zaworotko, M. J. *Chem. Commun.* **2003**, 1342. (d) Férey, G.;

Mellot-Draznieks, C.; Serre, C.; Millange, F.; Dutour, J.; Surblé., S.; Margiolaki, I. *Science* **2005**, *309*, 2040. (e) Chui, S. S. Y.; Lo, S. M. F.; Charmant, J. P. H; Orpen, A. G.; Williams, I. D. *Science* **1999**, *283*, 1148. (f) Bradshaw, D.; Prior, T. J.; Cussen, E. J.; Claridge, J. B.; Rosseinsky, M. J. *J. Am. Chem. Soc.* **2004**, *126*, 6106. (g) Chae, H. K.; Siberio-Pérez, D. Y.; Kim, J.; Go, Y.; Eddaoudi, M.; Matzger, A. J.; O'Keeffe, M.; Yaghi, O. M. *Nature* **2004**, *427*, 523. (h) Lin, X.; Jia, J.; Zhao, X.; Thomas, K. M.; Blake, A. J.; Walker, G. S.; Champness, N. R.; Hubberstey, P.; Schröder, M. *Angew. Chem., Int. Ed.* **2006**, *45*, 7358. (i) Lin, X.; Blake, A. J.; Wilson, C.; Sun, X. Z.; Champness, N. R.; George, M. W.; Hubberstey, P.; Mokaya, R.; Schröder, M. *J. Am. Chem. Soc.* **2006**, *128*, 10745. (j) Sava, D. F.; Kravtsov, V.; Nouar, F.; Wojtas, L.; Eubank, J. F.; Eddaoudi, M. *J. Am. Chem. Soc.* **2008**, *130*, 3768. (k) Caskey, S. R.; Wong-Foy, A. G.; Matzger, A. J. *J. Am. Chem. Soc.* **2008**, *130*, 10870.

(5) (a) Pigge, F. C. *CrystEngComm* **2011**, *13*, 1733. (b) Fletcher, A. J.; Thomas, K. M.; Rosseinsky, M. J. *J. Solid State Chem.* **2005**, *178*, 2491.

(6) Representative examples of MOFs using flexible ligands: (a) Zhao, X.; Xiao, B.; Fletcher, A. J.; Thomas, K. M.; Bradshaw, D.; Rosseinsky, M. J. *Science* **2004**, *306*, 1012. (b) Hawxwell, S. M.; Mínguez Espallargas, G.; Bradshaw, D.; Rosseinsky, M. J.; Prior, T. J.; Florence, A. J.; van de Streek, J.; Brammer, L. *Chem. Commun.* **2007**, 1532. (c) Yang, W.; Lin, X.; Blake, A. J.; Wilson, C.; Hubberstey, P.; Champness, N. R.; Schröder, M. *Inorg. Chem.* **2009**, *48*, 11067. (d) Qiu, W.; Perman, J. A.; Wojtas, Ł.; Eddaoudi, M.; Zaworotko, M. J. *Chem. Commun.* **2010**, *46*, 8734. (e) Xie, L.-H.; Suh, M. P. *Chem.—Eur. J.* **2011**, *17*, 13653. (f) Choi, H.-S.; Suh, M. P. *Angew. Chem., Int. Ed.* **2009**, *48*, 6865. (g) Rebilly, J.-N.; Bacsa, J.; Rosseinsky, M. J. *Chem.—Asian J.* **2009**, *4*, 892. (h) Ghosh, S. K.; Azhakar, R.; Kitagawa, S. *Chem.—Asian J.* **2009**, *4*, 870. (i) Hauptvogel, I. M.; Biedermann, R.; Klein, N.; Senkovska, I.; Cadiau, A.; Wallacher, D.; Feyerherm, R.; Kaskel, S. *Inorg. Chem.* **2011**, *50*, 8367. (j) Chun, H.; Seo, J. *Inorg. Chem.* **2009**, *48*, 9980.

(7) (a) Ferey, G.; Serre, C. *Chem. Soc. Rev.* **2009**, *38*, 1380. (b) Horike, S.; Shimomura, S.; Kitagawa, S. *Nat. Chem.* **2009**, *1*, 695.

(8) (a) Barthelet, K.; Marrot, J.; Riou, D.; Férey, G. *Angew. Chem., Int. Ed.* **2002**, *41*, 281. (b) Serre, C.; Millange, F.; Thouvenot, C.; Nogues, M.; Marsolier, G.; Louer, D.; Ferey, G. *J. Am. Chem. Soc.* **2002**, *124*, 13519. (c) Loiseau, T.; Serre, C.; Huguenard, C.; Fink, G.; Taulelle, F.; Henry, M.; Bataille, T.; Ferey, G. *Chem.—Eur. J.* **2004**, *10*, 1373. (d) Liu, Y.; Her, J. H.; Dailly, A.; Ramirez-Cuesta, A. J.; Neumann, D. A.; Brown, C. M. *J. Am. Chem. Soc.* **2008**, *130*, 11813. (e) Trung, T. K.; Trens, P.; Tanchoux, N.; Bourrelly, S.; Llewellyn, P. L.; Loera-Serna, S.; Serre, C.; Loiseau, T.; Fajula, F.; Férey, G. *J. Am. Chem. Soc.* **2008**, *130*, 16926. (f) Finsy, V.; Kirschhock, C. E.; Vedts, G.; Maes, M.; Alaerts, L.; De Vos, D. E.; Baron, G. V.; Denayer, J. F. *Chem.—Eur. J.* **2009**, *15*, 7724. (g) Walker, A. M.; Civalleri, B.; Slater, B.; Mellot-Draznieks, C.; Cora, F.; Zicovich-Wilson, C. M.; Roman-Perez, G.; Soler, J. M.; Gale, J. D. *Angew. Chem., Int. Ed.* **2010**, *49*, 7501. (h) Matsuda, R.; Kitaura, R.; Kitagawa, S.; Kubota, Y.; Kobayashi, T. C.; Horike, S.; Takata, M. *J. Am. Chem. Soc.* **2004**, *126*, 14063. (i) Salles, F.; Ghoufi, A.; Maurin, G.; Bell, R. G.; Mellot-Draznieks, C.; Férey, G. *Angew. Chem., Int. Ed.* **2008**, *47*, 8487. (j) Motkuri, R. K.; Thallapally, P. K.; Nune, S. K.; Fernandez, C. A.; McGrail, B. P.; Atwood, J. L. *Chem. Commun.* **2011**, *47*, 7077. (k) Thallapally, P. K.; Tian, J.; Radha Kishan, M.; Fernandez, C. A.; Dalgarno, S. J.; McGrail, P. B.; Warren, J. E.; Atwood, J. L. *J. Am. Chem. Soc.* **2008**, *130*, 16842. (l) Yang, C.; Wang, X.; Omary, M. A. *Angew. Chem., Int. Ed.* **2009**, *48*, 2500. (m) Millange, F.; Guillou, N.; Walton, R. I.; Grenèche, J.-M.; Margiolaki, I.; Férey, G. *Chem. Commun.* **2008**, 4732. (n) Kondo, A.; Kajiro, H.; Noguchi, H.; Carlucci, L.; Proserpio, D. M.; Ciani, G.; Kato, K.; Takata, M.; Seki, H.; Sakamoto, M.; Hattori, Y.; Okino, F.; Maeda, K.; Ohba, T.; Kaneko, K.; Kanoh, H. *J. Am. Chem. Soc.* **2011**, *133*, 10512. (o) Wang, X.; Eckert, J.; Liu, L.; Jacobson, A. J. *Inorg. Chem.* **2011**, *50*, 2028.

(9) (a) Chen, C.; Sun, J.-K.; Li, W.; Chen, C.-N.; Zhang, J. *Chem. Commun.* **2011**, *47*, 6683. (b) Ghosh, S. K.; Kaneko, W.; Kiriya, D.; Ohba, M.; Kitagawa, S. *Angew. Chem., Int. Ed.* **2008**, *47*, 8843. (c) Libri, S.; Mahler, M.; Mínguez Espallargas, G.; Singh, D. C. N. G.; Soleimannejad, J.; Adams, H.; Burgard, M. D.; Rath, N. P.; Brunelli, M.; Brammer, L. *Angew. Chem., Int. Ed.* **2008**, *47*, 1693. (d) Bradshaw, D.; Warren, J. E.; Rosseinsky, M. J. *Science* **2007**, *315*, 977. (e) Niel, V.; Thompson, A. L.; Muñoz, M. C.; Galet, A.; Goeta, A. E.; Real, J. A. *Angew. Chem., Int. Ed.* **2003**, *42*, 3760. (f) Mínguez Espallargas, G.; Brammer, L.; van de Streek, J.; Shankland, K.; Florence, A. J.; Adams, H. *J. Am. Chem. Soc.* **2006**, *128*, 9584. (g) Mínguez Espallargas, G.; Hippler, M.; Florence, A. J.; Fernandes, P.; van de Streek, J.; Brunelli, M.; David, W. I. F.; Shankland, K.; Brammer, L. *J. Am. Chem. Soc.* **2007**, *129*, 15606. (h) Mínguez Espallargas, G.; van de Streek, J.; Fernandes, P.; Florence, A. J.; Brunelli, M.; Shankland, K.; Brammer, L. *Angew. Chem., Int. Ed.* **2010**, *49*, 8892.

(10) (a) Coronado, E.; Giménez-Marqués, M.; Mínguez Espallargas, G.; Brammer, L. *Nat. Commun.* Accepted. (b) Kaneko, W.; Ohba, M.; Kitagawa, S. *J. Am. Chem. Soc.* **2007**, *129*, 13706. (c) Cheng, X.-N.; Zhang, W.-X.; Chen, X.-M. *J. Am. Chem. Soc.* **2007**, *129*, 15738. (d) Duan, Z.; Zhang, Y.; Zhang, B.; Zhu, D. *J. Am. Chem. Soc.* **2009**, *131*, 6934. (e) Hu, C.; Englert, U. *Angew. Chem., Int. Ed.* **2005**, *44*, 2281. (f) Ghosh, S. K.; Zhang, J.-P.; Kitagawa, S. *Angew. Chem., Int. Ed.* **2007**, *46*, 7965.

(11) Leong, W. L.; Vittal, J. J. *Chem. Rev.* **2011**, *111*, 688.

(12) (a) Lauher, J. W.; Fowler, F. W.; Goroff, N. S. *Acc. Chem. Res.* **2008**, *41*, 1215. (b) Halder, G. J.; Kepert, C. J. *Aust. J. Chem.* **2006**, *59*, 597. (c) Halasz, I. *Cryst. Growth Des.* **2010**, *10*, 2817.

(13) Vittal, J. J. *Coord. Chem. Rev.* **2007**, *251*, 1781.

(14) (a) Matsuda, R.; Kitaura, R.; Kitagawa, S.; Kubota, Y.; Belosludov, R. V.; Kobayashi, T. C.; Sakamoto, H.; Chiba, T.; Takata, M.; Kawazoe, Y.; Mita, Y. *Nature* **2005**, *436*, 238. (b) Kawano, M.; Haneda, T.; Hashizume, D.; Izumi, F.; Fujita, M. *Angew. Chem., Int. Ed.* **2008**, *47*, 1269. (c) Ohara, K.; Martí-Rujas, J.; Haneda, T.; Kawano, M.; Hashizume, D.; Izumi, F.; Fujita, M. *J. Am. Chem. Soc.* **2009**, *131*, 3860. (d) Fujii, K.; Lazuen Garay, A.; Hill, J.; Sbircea, E.; Pan, Z.; Xu, M.; Apperley, D. C.; James, S. L.; Harris, K. D. M. *Chem. Commun.* **2010**, *46*, 7572. (e) Martí-Rujas, J.; Islam, N.; Hashizume, D.; Izumi, F.; Fujita, M.; Jae Song, H.; Choi, H. C.; Kawano, M. *Angew. Chem., Int. Ed.* **2011**, *50*, 6105. (f) Martí-Rujas, J.; Islam, N.; Hashizume, D.; Izumi, F.; Fujita, M.; Kawano, M. *J. Am. Chem. Soc.* **2011**, *133*, 5853.

(15) Rabone, J.; Yue, Y.-F.; Chong, S. Y.; Stylianou, K. C.; Bacsa, J.; Bradshaw, D.; Darling, G. R.; Berry, N. G.; Khimyak, Y. Z.; Ganin, A. Y.; Wiper, P.; Claridge, J. B.; Rosseinsky, M. J. *Science* **2010**, *329*, 1053.

(16) (a) Maspoch, D.; Ruiz-Molina, D.; Veciana, J. *J. Mater. Chem.* **2004**, *14*, 2713. (b) Dechambenoit, P.; Long, J. R. *Chem. Soc. Rev.* **2011**, *40*, 3249. (c) Halder, G. J.; Kepert, C. J.; Moubaraki, B.; Murray, K. S.; Cashion, J. D. *Science* **2002**, *298*, 1762. (d) Ohba, M.; Yoneda, K.; Agustí, G.; Muñoz, M. C.; Gaspar, A. B.; Real, J. A.; Yamasaki, M.; Ando, H.; Nakao, Y.; Sakaki, S.; Kitagawa, S. *Angew. Chem., Int. Ed.* **2009**, *48*, 4767. (e) Agustí, G.; Ohtani, R.; Yoneda, K.; Gaspar, A. B.; Ohba, M.; Sánchez-Royo, J. F.; Muñoz, M. C.; Kitagawa, S.; Real, J. A. *Angew. Chem., Int. Ed.* **2009**, *48*, 8944. (f) Kurmoo, M.; Kumagai, H.; Chapman, K. W.; Kepert, C. J. *Chem. Commun.* **2005**, 3012. (g) Motokawa, N.; Matsunaga, S.; Takaishi, S.; Miyasaka, H.; Yamashita, M.; Dunbar., K. R. *J. Am. Chem. Soc.* **2010**, *132*, 11943.

(17) *Magneto-Structural Correlations in Exchange Coupled Systems*; Willett, R. D., Gatteschi, D., Kahn, O., Eds.; Reidel: Dordrecht, The Netherlands, 1985; p 241.

(18) Meng, X.; Song, Y.; Hou, H.; Han, H.; Xiao, B.; Fan, Y.; Zhu, Y. *Inorg. Chem.* **2004**, *43*, 3528.

(19) Sheldrick, G. M. *Acta Crystallogr., Sect. A: Found. Crystallogr.* **2008**, *64*, 112.

(20) (a) Liu, K.; Shi, W.; Cheng, P. *Dalton Trans.* **2011**, *40*, 8475. (b) Li, B.; Peng, Y.; Li, B.; Zhang, Y. *Chem. Commun.* **2005**, 2333. (c) Meng, X.; Liu, Y.; Song, Y.; Hou, H.; Fan, Y.; Zhu, Y. *Inorg. Chim. Acta* **2005**, *358*, 3024. (d) Li, B.; Peng, Y.; Liu, X.; Li, B.; Zhang, Y. *J. Mol. Struct.* **2005**, *741*, 235. (e) Peng, Y.-F.; Ge, H.-Y.; Li, B.-Z.; Li, B.-L.; Zhang, Y. *Cryst. Growth Des.* **2006**, *16*, 994. (f) Du, J.-L.; Hu, T.-L.; Zhang, S.-M.; Zeng, Y.-F.; Bu, X.-H. *CrystEngComm* **2008**, *10*, 1866.

(g) Chen, Y.; Zhang, S.-Y.; Zhao, X.-Q.; Zhang, J.-J.; Shi, W.; Cheng, P. *Inorg. Chem. Commun.* **2010**, *13*, 699.
(21) Zhang, S.-Y.; Zhang, Z.-J.; Shi, W.; Zhao, B.; Cheng, P.; Liao, D.-Z.; Yan, S.-P. *Dalton Trans.* **2011**, *40*, 7993.
(22) Removal of coordinated water molecules below 100 °C has been reported in the literature: (a) Ranford, J. D.; Vittal, J. J.; Wu, D. *Angew. Chem., Int. Ed.* **1998**, *37*, 1114. (b) Ranford, J. D.; Vittal, J. J.; Wu, D.; Yang, X. *Angew. Chem., Int. Ed.* **1999**, *38*, 3498. (c) Campo, J.; Falvello, L. R.; Mayoral, I.; Palacio, F.; Soler, T.; Tomás, M. *J. Am. Chem. Soc.* **2008**, *130*, 2932. (d) Bardelang, D.; Udachin, K. A.; Anedda, R.; Moudrakovski, I.; Leek, D. M.; Ripmeester, J. A.; Ratcliffe, C. I. *Chem. Commun.* **2008**, 4927. (e) Dietzel, P. D. C.; Johnsen, R. E.; Blom, R.; Fjellvåg, H. *Chem.—Eur. J.* **2008**, *14*, 2389. (f) Duan, Z.; Zhang, Y.; Zhang, B.; Zhu, D. *J. Am. Chem. Soc.* **2009**, *131*, 6934. (g) Kawasaki, T.; Hakoda, Y.; Mineki, H.; Suzuki, K.; Soai, K. *J. Am. Chem. Soc.* **2010**, *132*, 2874. (h) Ling, Y.; Zhang, L.; Lia, J.; Du, M. *CrystEngComm* **2011**, *13*, 768.
(23) Lu, J.; Paliwala, T.; Lim, S. C.; Yu, C.; Niu, T.; Jacobson, A. J. *Inorg. Chem.* **1997**, *36*, 923.
(24) (a) Banci, L.; Bencini, A.; Benelli, C.; Gatteschi, D.; Zanchini, C. Spectral-Structural Correlations in High-Spin Cobalt(II) Complexes. *Structure & Bonding*; Springer-Verlag: Berlin, Germany, 1982; Vol. *52*, pp 37−86. (b) Abragam, A.; Pryce, M. H. L. *Proc. R. Soc. London A* **1951**, *206*, 173.
(25) It should be noted that the reaction times are surface area dependent, so the well-packed sample used in this experiment results in an increase in the reaction time for completion.